Int J Thermophys (2010) 31:1979–1990
DOI 10.1007/s10765-008-0496-8

Thermophysical Properties of Ceramic Filler-Added $BaO–ZnO–B_2O_3–P_2O_5$ Glass Composites for Barrier Ribs of Plasma Display Panels

Eugene Chong · Seongjin Hwang · Wookyung Sung · Hyunho Shin · Hyungsun Kim

Published online: 12 August 2008

Abstract The capability of $BaO–ZnO–B_2O_3–P_2O_5$ glass in hosting various ceramic fillers (up to 20 mass% of Al_2O_3, TiO_2, and ZnO) has been investigated. All the investigated filler-added glasses have demonstrated a reasonable densification at 550 °C to form stable ceramic filler-glass composites. Modifications of the thermophysical properties, such as coefficient of thermal expansion (CTE), glass transition temperature, and dilatometric softening temperature, by the addition of the fillers have been investigated and correlated to phase and microstructural evolution. The CTE of the fabricated composites with varying filler addition is well correlated with theoretical predictions based on the Turner equation considering the modification by phase evolution, which indicates the thermal property tuning potential of the BZBP-based glass composites for application to barrier ribs of plasma display panels.

Keywords Barium zinc borophosphate glass · Barrier rib · Coefficient of thermal expansion · Crystallization temperature · Fillers · Glass transition temperature · Microstructure · Thermal Properties

1 Introduction

Barrier rib materials of plasma display panels (PDPs) are composites composed of refractory ceramic fillers and a low-melting glass matrix. These composites are often used instead of homogeneous materials because their physical properties (such as

E. Chong · S. Hwang · W. Sung · H. Kim (✉)
School of Materials Engineering, Inha University, Incheon 402-751, Republic of Korea
e-mail: kimhs@inha.ac.kr

H. Shin
Department of Ceramic Engineering, Kangnung National University, Kangnung 210-702, Republic of Korea

optical reflectance, dielectric constant, and coefficient of thermal expansion) are suitably tuned. In order to enable the glass matrix to host various types of refractory ceramic fillers, it is important during the development of the composites that sintering be conducted at a reasonably low processing temperature, e.g., 550 °C, with a strong interfacial bond between the filler and the matrix. Conventionally, lead oxide-containing borosilicate glasses have been used for the matrix of the barrier ribs [1,2] because of their good hosting capability of refractory ceramic fillers, low-softening temperature, comparable CTE to aluminum borosilicate glass panels such as PD200 (8.3×10^{-6} K^{-1}; Asahi Glass, Tokyo, Japan), low dielectric constant, and high optical reflectance. Because of the deleterious influence of PbO on health and environment during processing, there has been much work to avoid the use of PbO constituents. Some of the notable alternative glasses are the recently reported BaO–ZnO–B_2O_3 [3] and BaO–ZnO–B_2O_3–SiO_2 [4–7] systems.

In an effort toward developing a new BaO–ZnO–B_2O_3–P_2O_5 glass system for the matrix of the barrier ribs, here we report the capability of one BaO–ZnO–B_2O_3–P_2O_5 glass formulation in hosting various ceramic fillers (up to 20 mass% of Al_2O_3, TiO_2, and ZnO), and report how the thermophysical properties (such as CTE, glass transition point (T_g), and dilatometric softening point (T_d) of the fabricated composites) can be tailored by the addition of the ceramic fillers. Property modifications have been correlated to phase and microstructural evolutions by the filler additions.

2 Experimental Procedure

BZBP glass was fabricated by mixing BaO (99.9 %, Aldirich Chemical Co., Delaware, USA), ZnO (99.9 %, Aldirich Chemical Co., Delaware, USA), B_2O_3 (99.9 %, Aldirich Chemical Co., Delaware, USA), and P_2O_5 (99.9 %, Aldirich Chemical Co., Delaware, USA) powders, ball-milling in air using zirconia balls, drying, melting at 1,300 °C for 1 h, and finally quenching to a metallic mold. The quenched glass was pulverized to an average particle size of 1.0 µm using a planetary mono mill (Fritsch, Pulverisette-7, Germany) with zirconia balls and container.

The BZBP glass frits were mixed with three types of fillers: TiO_2 (rutile, avg. particle size of 2 µm, high purity, Chemicals, Saitama, Japan), Al_2O_3 (alpha alumina, avg. particle size of 2–3 µm, high purity, Chemicals, Saitama, Japan), and ZnO (avg. particle size of 2–3 µm, high purity, Chemicals, Saitama, Japan) using a Turbula mixer (Glen Mills Inc., Model T2F, Switzerland) with zirconia balls and container. The mixture powder was then uniaxially pressed into a disk shape at $\sim$1.3 kgf $\cdot$ cm^{-2}, followed by densification at 550 °C for 30 min in air.

The glass transition temperature (T_g) and onset point of crystallization (T_c) were determined using a differential thermal analyzer (DTA, TG 8120, Rigaku Co, Japan) at a heating rate of 10 °C $\cdot$ min^{-1}. Crystalline phases in the fabricated composites were identified by X-ray diffraction (XRD, Rigaku, Model DMAX-2500, Japan) using K radiation. The CTE of the specimens was measured using a horizontal-loading dilatometer (Netzch Instruments, Model DIL 402PC, Germany). The microstructure of the residual ceramic fillers in the glass-ceramic composites was investigated by

scanning electron microscopy (SEM Hitachi, Japan) using the back scattering mode after polishing under 1 μm with a diamond paste.

3 Results and Discussion

3.1 Properties of BZBP Matrix Glass

Thermal properties of the BZBP matrix glass were first investigated by dilatometry and differential thermal analysis (DTA), and the results are shown in Figs. 1 and 2. In Fig. 1, the glass transition point and dilatometric softening point of the BZBP glass have been checked, since these factors are important for the manufacturing of the PDP

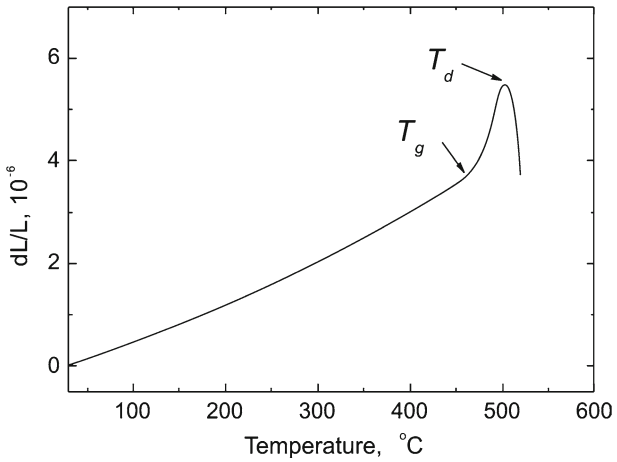

Fig. 1 Thermal expansion of the BZBP matrix glass with rising temperature

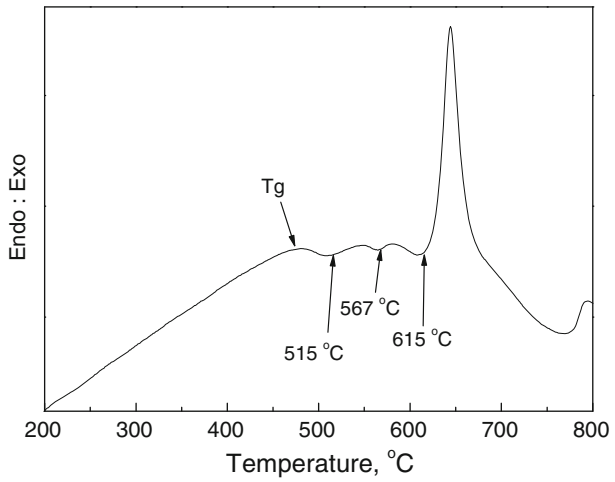

Fig. 2 DTA of the BZBP matrix glass

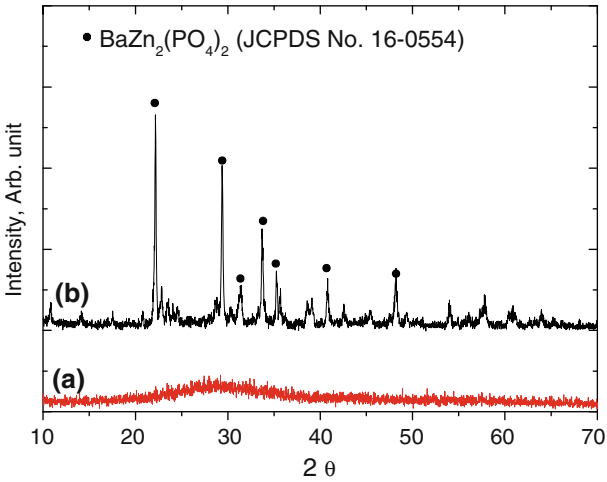

Fig. 3 XRD traces of the BZBP matrix glass frits after sintering at (a) 570 °C and (b) 630 °C

system. The glass transition point (T_g) determined at the temperature where the slope of the expansion curve (dL/L where L is the length of the specimen) deviates from linearity is 457 °C and the dilatometric softening point (T_d) recorded at the temperature where the expansion curve is a maximum is 502 °C. These properties are suitable for the fabrication of the PDP system at ∼550 °C.

DTA of the matrix glass (Fig. 2) shows a primary exothermic peak starting at 615 °C, at which the $BaZn_2(PO_4)_2$ phase appears, as identified by XRD as shown in Fig. 3. The fluctuation of the DTA trace at temperatures lower than 615 °C is interpreted to be due to the formation of the submicroscopic nuclei of the crystals because: (1) the glass changed to a weakly opaque state after the thermal treatment in the corresponding temperature range (data not shown in this paper: light scattering by submicroscopic nuclei), and (2) the thermal treatment did not yield any identifiable crystalline phases in XRD as seen in Fig. 3. Thus, 515 °C and 567 °C, marked in Fig. 2, are interpreted to be the starting temperatures of the broad exothermic peaks for the formation of submicroscopic nuclei.

3.2 Phase and Microstructural Evolution by Filler Additions

Crystalline phases in the fabricated composites have been identified by XRD (Fig. 4), as they are among the key factors in explaining the properties of the fabricated composites. In Fig. 4a, peak intensities of TiO_2 increase with the addition of TiO_2 up to 15 mass%, while at 20 mass% addition, the formation of the $BaZn_2(PO_4)_2$, $BaTiO_3$, and ZnO phases is so apparent that the TiO_2 peaks almost disappear; a crystalline composite of $BaZn_2(PO_4)_2$, $BaTiO_3$, and ZnO forms, while the $BaZn_2(PO_4)_2$ phase turns out to be the most dominant at this composition. The formation of the ZnO second phase is observed only when TiO_2 is added, whereas the $BaZn_2(PO_4)_2$ phase appears for the cases of Al_2O_3 and ZnO filler additions as well. It is well known that various

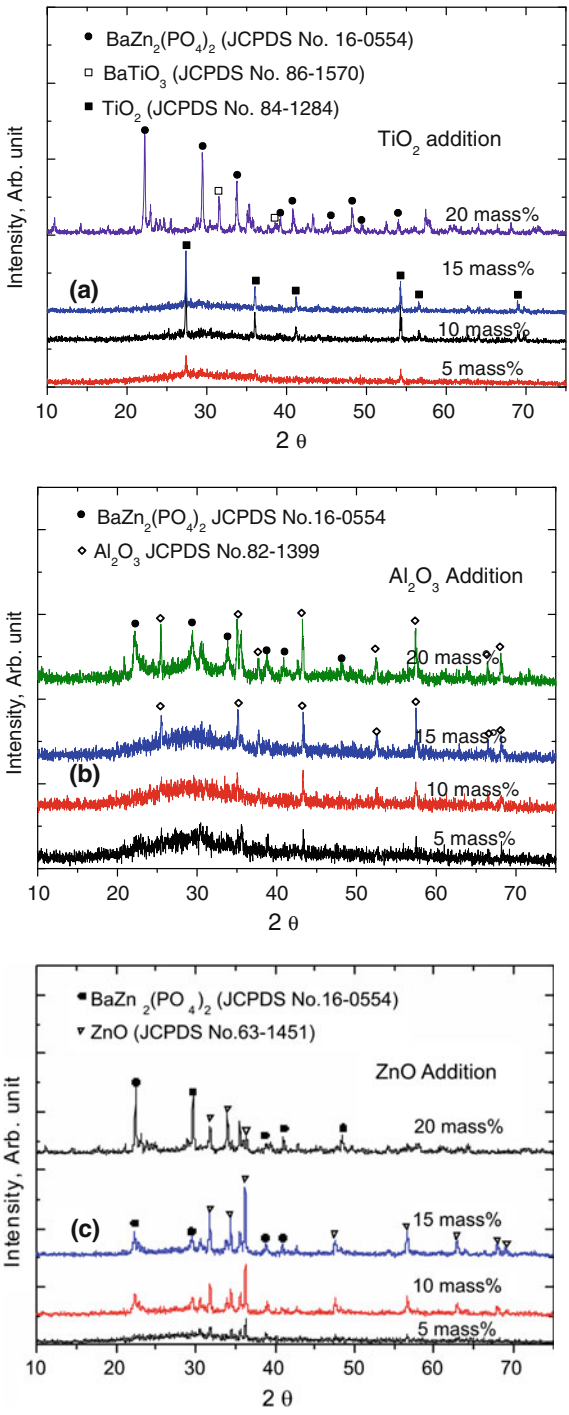

Fig. 4 XRD traces of (**a**) TiO_2, (**b**) Al_2O_3, and (**c**) ZnO filler-added composites with varying filler amount (fabricated at 550 °C)

refractory ceramic fillers such as TiO_2, Al_2O_3, ZrO_2, MgO, and cordierite are partially dissolved in a low-melting glass such as barium zinc borosilicate glass [4–7]. Such partial dissolution of the fillers would also be the case herein in the BZBP glass matrix. The partially dissolved TiO_2 in the BZBP matrix would then modify the glass composition to lower the solubility limit of ZnO for precipitate formation.

For the case of Al_2O_3 addition (Fig. 4b), the peak intensities of Al_2O_3 also increase up to 15 mass% addition, while at 20 mass% addition, the $BaZn_2(PO_4)_2$ phase newly appears so that the crystalline composite of Al_2O_3 and $BaZn_2(PO_4)_2$ forms. As for ZnO addition (Fig. 4c), the formation of the $BaZn_2(PO_4)_2$ phase is so apparent that it appears from the 10 mass% ZnO addition to form a crystalline composite of ZnO and $BaZn_2(PO_4)_2$. At 20 mass% addition, the $BaZn_2(PO_4)_2$ phase turns out to be the primary phase.

Microstructures of the 15 mass%-added filler for three types of the specimens are shown in Fig. 5. Corresponding phases to the XRD result are identified in the microstructure by energy dispersive spectroscopy (data not shown) and are marked in Fig. 5. The fillers are well dispersed and no appreciable interfacial gap between the fillers and the glass matrix exists. For TiO_2 and Al_2O_3-added composites, only added filler morphologies are identified at 15 mass% addition, while for the ZnO-added case, the additional $BaZn_2(PO_4)_2$ phase is identified. These findings are all consistent with the XRD observation (Fig. 4).

3.3 Properties of the Filler-Added Composites

Changes in T_g and T_d by the filler addition to the glass matrix have been investigated, and the results are shown in Fig. 6. In Fig. 6a, T_g's of TiO_2 and Al_2O_3 filler-added specimens vary by a relatively small amount as compared to those for ZnO-filler addition. T_g is modified due to the change in the composition of the glass matrix as the refractory ceramic fillers are partially dissolved in similar low-melting glasses [5]. T_g of 15–20 mass% ZnO-added composites is higher than the glass matrix by ~20 °C, possibly due to the more enhanced ZnO dissolution into the glass matrix. However, this increase in T_g by ZnO addition is much smaller than the increase in T_d by the filler additions (Fig. 6b) because T_g is the property of the glass matrix itself, which is only influenced by its subtle compositional change due to the partially dissolved fillers, while T_d is influenced directly by the presence of refractory fillers.

When TiO_2 and Al_2O_3 fillers are added, T_d is more or less similar up to 15 mass% additions, followed by drastic increases at 20 mass% addition. These drastic increases in T_d are well correlated to the formation of secondary phases at 20 mass% filler additions, i.e., $BaZn_2(PO_4)_2$ and ZnO for TiO_2 addition, and $BaZn_2(PO_4)_2$ for Al_2O_3 addition (Fig. 4). For the case of ZnO-filler addition, a drastically increased T_d appears from about 10 mass% addition, which is again well correlated to the XRD observation that the $BaZn_2(PO_4)_2$ second phase appears from 10 mass% addition of ZnO. An interesting point in ZnO-added composites is that the significantly increased T_g appears from 15 mass% ZnO, while the increase in T_d starts at 10 mass% addition. This increase may arise because T_g is influenced by the change in glass composition due to the partial dissolution of ZnO, while T_d is governed by the crystalline phases, as noted above.

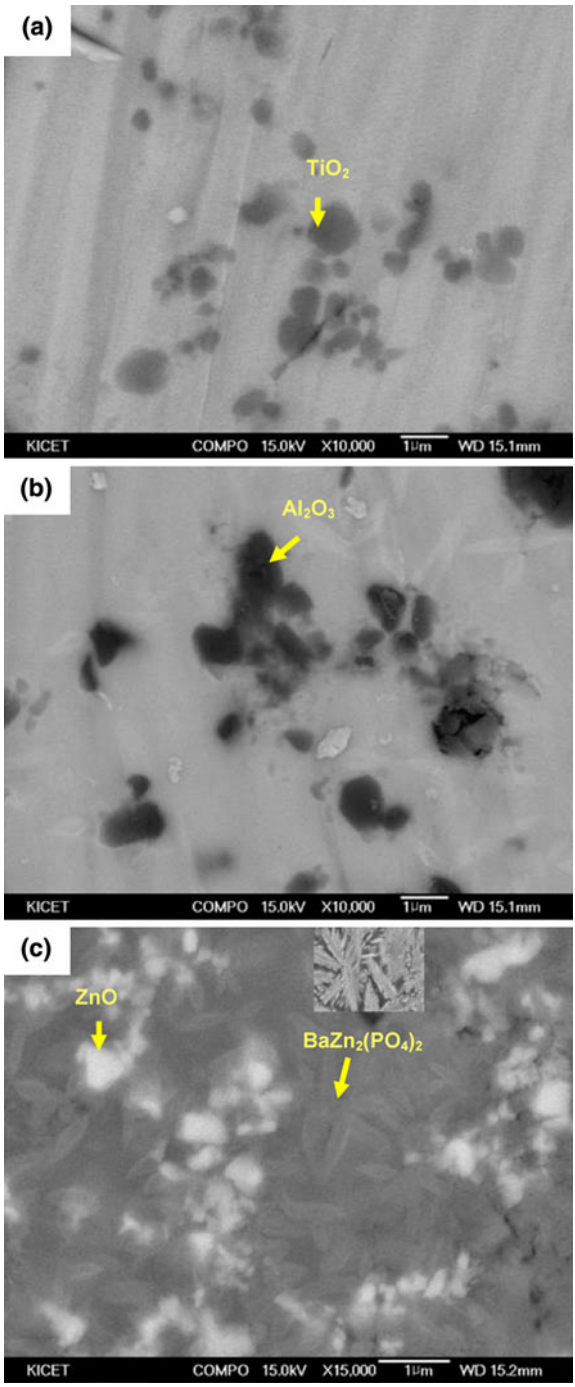

Fig. 5 Microstructure of the 15 mass% filler-added BZBP glass matrix composites: (**a**) TiO_2, (**b**) Al_2O_3, and (**c**) ZnO

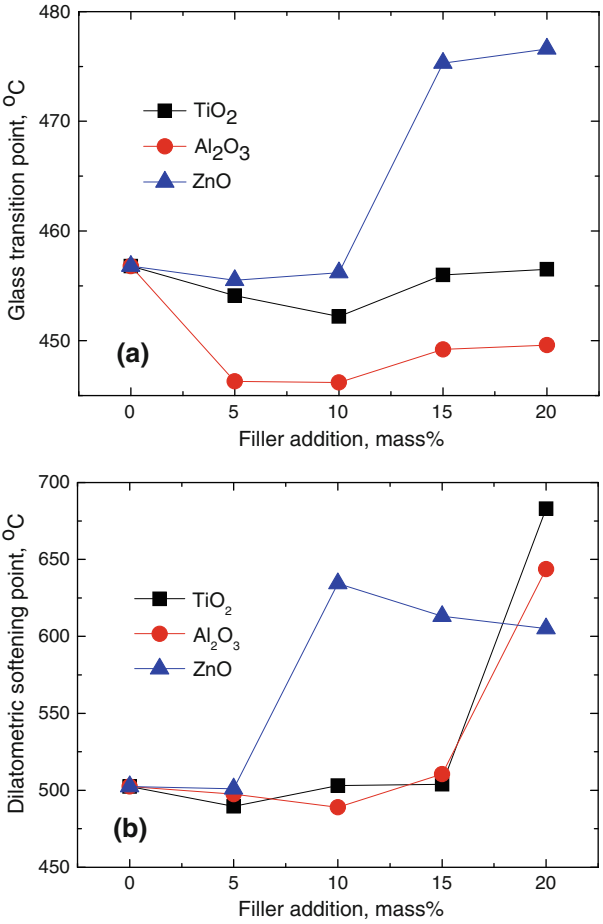

Fig. 6 Changes in (**a**) glass transition point and (**b**) dilatometric softening point of the fabricated composites as functions of filler addition for thes three types of fillers

The relative density of the fabricated composites has been investigated to check the successful fabrication of the composites (the result is shown in Fig. 7) based on the assumption that glass and refractory fillers do not react during sintering. TiO_2 and Al_2O_3 filler-added specimens demonstrate fairly high relative density (higher than 96 % up to 20 mass% additions), while ZnO-filler addition yields smaller densification. The partially dissolved ZnO in the glass matrix is interpreted to increase the viscosity of the glass matrix unlike TiO_2 and Al_2O_3, which resists the densification of the ZnO-added composites. This view corresponds to the higher T_g of the ZnO-filler added composites (especially from 15 mass% additions) than for other filler-glass composites (Fig. 6a).

Having shown the hosting capability of the BZBP glass for the three types of fillers, the changes in the CTE of the fabricated composites are investigated, and the result is shown in Fig. 8 as a function of the filler addition. Included in Fig. 8 are the predicted

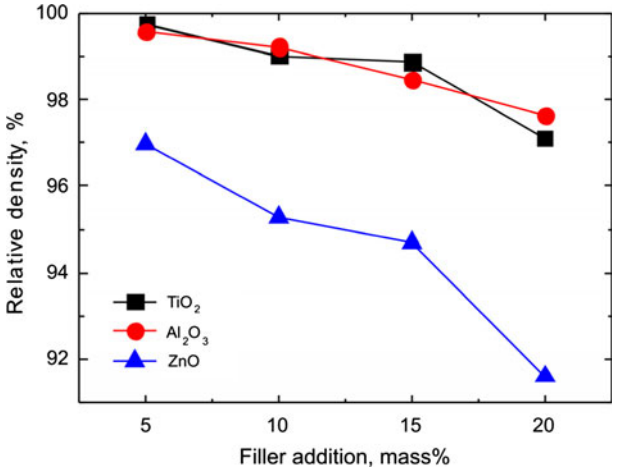

Fig. 7 Change in relative density as a function of filler addition for the three types of filler

values by the Turner equation [8],

$$\alpha_c = \frac{\alpha_g V_g K_g + \alpha_f V_f K_f}{V_g K_g + V_g K_f},$$

where α is the CTE, V the volume fraction, K the bulk modulus ($= E/3(1-2\nu)$ where E is the elastic modulus and ν is Poisson's ratio), and subscripts g, f, and c denote the glass matrix, filler, and composite, respectively. The properties of the materials used for the calculation are shown in Table 1.

The addition of TiO_2 filler yields CTE values corresponding to the predicted ones up to 15 mass%, while a decrease from the predicted value is noted at 20 mass% addition, possibly due to the secondary crystalline mixture of $BaZn_2(PO_4)_2$, $BaTiO_3$, and ZnO at 20 mass%. For the case of Al_2O_3 addition, consistent results between experiment and theory are also observed up to 15 mass% addition, while deviations from the predicted values are apparent thereafter. These deviations can be correlated to the formation of the second phase $BaZn_2(PO_4)_2$, which might possess a lower CTE than Al_2O_3, at 20 mass% addition of Al_2O_3. Since the amount of partially dissolved fillers increases as the filler addition increases [4–7], the increased alteration of the glass property at 20 mass% addition of TiO_2 and Al_2O_3 would also contribute to deviations from the predictions.

For the case of ZnO addition, the influence of the alteration of glass properties due to the partial dissolution of filler seems to be the most pronounced. When ZnO filler is added, the experimental CTE is fairly consistent with predictions up to 10 mass% addition: it decreases monotonically with ZnO addition due to the fairly low CTE of ZnO ($2.8 \times 10^{-6}\,K^{-1}$) up to 10 mass% ZnO. However, higher CTE values than those from theories are recorded from 15 mass% addition. Judging solely from the crystalline phase evolution, any discrepancy from theory has to be observed from 10 mass%

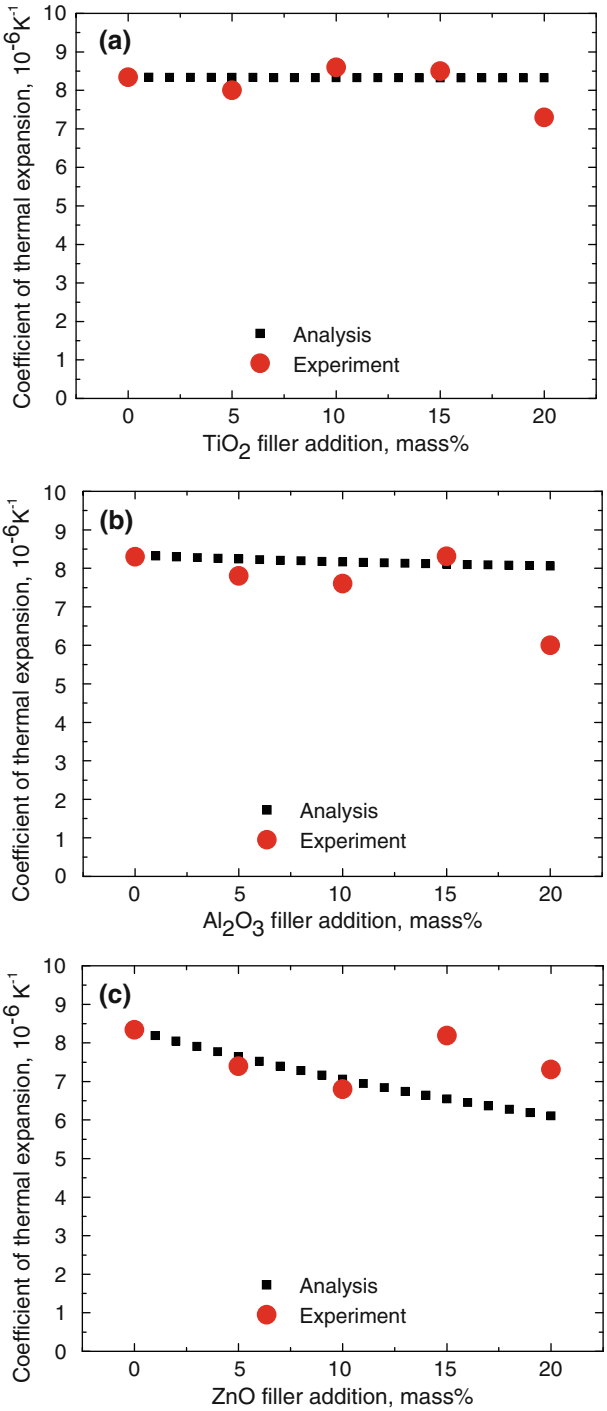

Fig. 8 Change in CTE of the composites as a function of filler addition: (**a**) Al_2O_3, (**b**) TiO_2, and (**c**) ZnO

Table 1 Properties of materials used for the calculation of the CTE of the composites by Turner equation

Material	Poisson ratio	Young's modulus (GPa)	CTE ($10^{-6}\,K^{-1}$)
TiO_2[a]	0.27	230	8.3
Al_2O_3[a]	0.22	379	7.8
ZnO	0.25[a]	220[b]	2.9[a]
BZBP glass	0.27[c]	73[d]	8.34[e]

[a] Reference [9]
[b] Extrapolated to pore-free ZnO value in Ref. [10]
[c] Poisson ratio of the B_2O_3-rich borosilicate glasses [11] are used
[d] Calculated by the Makeshida and Mackenzie model [12] using density of $3.805\,g\cdot cm^{-3}$
[e] Measured in the current work

addition instead of 15 mass% addition because the second phase $BaZn_2(PO_4)_2$, which might possess a higher CTE than ZnO, newly appears from 10 mass% addition.

Note, however, that evidence for the significant partial dissolution of ZnO in the glass matrix has been found: a drastic increase of T_g from 15 mass% ZnO addition instead of 10 mass% addition. Furthermore, the fact that ZnO is no longer the primary crystalline phase at 20 mass% also supports the view of a significant partial dissolution of ZnO in the glass matrix. Thus, the deviations of CTE from theory from 15 mass% ZnO addition, instead of 10 mass% addition (where the second phase appears), are interpreted to be due to the significantly altered glass properties induced by the partially dissolved ZnO into the glass matrix.

4 Conclusions

Al_2O_3, TiO_2, and ZnO ceramic fillers proved to form stable ceramic filler-added composites with reasonable relative densities (higher than 96 % up to 20 mass% addition of TiO_2 and Al_2O_3 and higher than 92 % for the case of 20 mass% ZnO addition). Modifications of the thermophysical properties (such as CTE, glass transition temperature, and dilatometric softening temperature) have been investigated by the addition of the fillers, and the modifications were correlated to phase and microstructural evolution. The CTE of the fabricated composites was well correlated with the Turner equation when the amount of filler addition was small. At higher filler additions, deviations from the predicted values were observed, which has been interpreted in terms of the formation of the second phases and compositional modification of the glass matrix by the partial dissolution of the fillers. Furthermore, the glass transition point and dilatometric softening point are shown to be tailored significantly by the filler addition to the investigated glass system, which was also influenced by the filler dissolution and formation of the second phase. These observations indicate the tuning potential of the thermophysical properties of BZBP-based glass composites for application to barrier ribs of PDPs.

Acknowledgments This work was partially supported by the Ministry of Education and Human Resources Development (MOE), the Ministry of Commerce, Industry and Energy (MOCIE), and the Ministry of Labor

(MOLAB) through the fostering project of the Lab of Excellency, and was supported by the Ministry of Commerce, Industry and Energy (MOCIE) through the New Growth Engine Project.

References

1. J.H. Jean, S.C. Lin, S.L. Yang, J. Appl. Phys. **34**, L422 (1995)
2. G.H. Hwang, H.J. Jeon, Y.S. Kim, J. Am. Ceram. Soc. **85**, 2961 (2002)
3. D.N. Kim, J.Y. Lee, J.S. Huh, H.S. Kim, J. Non-Cryst. Solids **306**, 70 (2002)
4. S.G. Kim, H. Shin, J.S. Park, K.S. Hong, H. Kim, J. Electroceram. **15**, 129 (2005)
5. S.G. Kim, J.S. Park, J.S. An, K.S. Hong, H. Shin, H. Kim, J. Am. Ceram. Soc. **89**, 902 (2006)
6. H. Shin, S.G. Kim, J.S. Park, J.S. An, K.S. Hong, H. Kim, J. Am. Ceram. Soc. **89**, 3258 (2006)
7. H. Shin, J.S. Park, S.G. Kim, H.S. Jung, K.S. Hong, H. Kim, J. Mater. Res. **21**, 1753 (2006)
8. P.S. Turner, J. Res. Nat. Bur. Stand. **37**, 239 (1946)
9. MatWeb, Material Property Data. http://www.matweb.com
10. A.K. Mukhopadhyay, M.R. Chaudhuri, A. Seal, S.K. Dalui, M. Banerjee, K.K. Phani, Bull. Mater. Sci. **24**, 125 (2001)
11. J.F. Shackelford, W. Alexander, J.S. Park, *CRC Materials Science and Engineering Handbook*, 2nd edn. (CRC Press, London, 1994), p. 540
12. A. Makishima, J.D. Mackenzie, J. Non-Cryst. Solids. **12**, 35 (1973)